

Size distribution and organ development of the hooded oyster, *Saccostrea cucullata* (Born, 1778) from Libong Island, Thailand

Kitiya Kongthong^a, Sinlapachai Senarat^b, Anjaree Inchan^c, Gen Kaneko^d, Atsuo Iida^e, Ittipon Phoungpetchara^f, Natthawut Charoenphon^{f,*}

^a Faculty of Medical Science, Naresuan University, Phitsanulok 65000 Thailand

^b Division of Biological Science, Faculty of Science, Prince of Songkla University, Songkhla 90110 Thailand

^c Department of Physiology, Faculty of Medical Science and Center of Excellence for Innovation in Chemistry, Naresuan University, Phitsanulok 65000 Thailand

^d College of Natural and Applied Science, University of Houston-Victoria, Victoria, TX 77901 USA

^e Department of Animal Sciences, Graduate School of Bioagricultural Sciences, Nagoya University, Nagoya 464-8601 Japan

^f Department of Anatomy, Faculty of Medical Science, Naresuan University, Phitsanulok 65000 Thailand

*Corresponding author, e-mail: natthawutch@nu.ac.th

Received 4 Jun 2023, Accepted 22 Sep 2023

Available online 29 Dec 2023

ABSTRACT: The hooded oyster, *Saccostrea cucullata*, is an economically important bivalve in Thailand with great potential for aquaculture production. Since its histological development remains unknown, we examined the organ development of field-collected *S. cucullata* associated with their shell size distributions from Libong Island, Thailand. The water quality parameters were not significantly different between the sampling areas except for the water temperature ($p < 0.05$). *S. cucullata* from the Stone Bridge (SB) site had smaller shell lengths and higher condition factors than those from Dugong Tourism by Drones (DT) except for the size of the organ. Histologically, the highest mean length of gill lamellae was $192.1 \pm 3.92 \mu\text{m}$ in 2.1–3 cm group. The thinnest of the mantle epithelium ($73.78 \pm 3.08 \mu\text{m}$ in 4.1–5 cm group) of *S. cucullata* showed statistically significant difference between the sampled locations (Specific F value = 0.1783 and 0.8605 when $p < 0.01$ and $p < 0.0001$, respectively). The density of mucous-secreting cells (Msc) was more prominently distributed in the digestive gland than in other tissues. The 2.1–3 cm group or bigger had mature gonads with protandric characteristics, showing the rapid sexual differentiation in SB. Results obtained from this study improve the current knowledge of *S. cucullata* from natural environments, which potentially contributes to the establishment of its aquaculture.

KEYWORDS: histological analysis, functional organs, morphometric analysis, mucous-secreting cells, the hooded oyster

INTRODUCTION

The size distribution of aquatic invertebrates is an important indicator of their community and ecosystem structure [1]. The size distribution of aquatic invertebrates is easy to determine from field observations, so this has been used to estimate the growth and metabolic rate in various aquatic invertebrates as the reflection of their physiological activity and life history under specific ecological conditions [1]. For example, Fey et al [2] showed that the growth of the Pacific oyster *Crassostrea gigas* differs depending on the locations and seasons in the subtidal and intertidal areas from the north of the Netherlands to Denmark, as similarly reported by Kang et al [3] in their Korean study. The size distribution data becomes more useful when it is reported with histological analysis that can detect maturation status and the degree of environmental stress. Davenel et al [4] monitored the gonadal development of *Ostrea edulis* under laboratory conditions, showing significant development before spawning. *Striostrea prismatica* collected from

the southern coast of Ecuador showed an increase in oocyte diameter and the follicular layer area in the spawning season [5]. On the other hand, the growth of oysters is negatively regulated by pathogens and environmental stressors. Wang et al [6] suggested that high temperatures can increase the risk of *Vibrio parahaemolyticus* infection in *Crassostrea rivularis*, resulting in a decline in growth rate and increased mortality.

The hooded oyster *Saccostrea cucullata* (Born, 1778), belonging to the family Ostreidae, is a commonly observed species on the coast of Thailand as well as the tropical Indo-West Pacific area [7]. This species has a huge potential for increasing its aquaculture production [8] and has been actively studied for its taxonomy, morphological features [7], gamete characteristics [9], and the optimum temperature of 20–30 °C [10]. However, the histological development of *S. cucullata* in the natural environment remains unknown. We therefore examined the histological development of *S. cucullata* about the shell size distribution at different locations in Libong Island, Thailand.

MATERIALS AND METHODS

Oyster collection and study sites

Hooded oysters, *Saccostrea cucullata* ($n = 50$ per location), were field collected in April 2022 at 2 locations in Libong Island, Thailand, including Stone Bridge (SB, $7^{\circ}16'17.9''$ N $99^{\circ}22'38.3''$ E). At locations close to the sand beach, there was minor life-threatening human activity [11]. However, close to the seagrass beds near the Dugong Tourism by Drones site (DT, $7^{\circ}13'20.6''$ N $99^{\circ}24'08.3''$ E), there was major life-threatening tourist activity [11]. The water quality parameters, including dissolved oxygen (DO), water temperature, pH, salinity, and turbidity, were measured at each location using a multi-parameter water quality meter (HORIBA, Japan). The live specimens were transferred to the Histology Laboratory at the Medical Science Academic Service Centre (Standard laboratory in Number 2-0100-0004-8), Faculty of Medical Science, Naresuan University. Species were identified based on the taxonomic guideline of Cardoso et al [12], and the *S. cucullata* individuals were euthanized with a rapid cooling shock [13]. This study was approved by the Naresuan University Animal Care and Use Committee under process number NU-AQ650303.

Gross anatomy and morphometric analysis

Gross anatomy and morphometric parameters were examined following the standard guideline from the OIE Diagnostic Manual for Diseases of Aquatic Animals [14]. The anterior valve was photographed with a digital camera (Sony A6000, Japan). The shell length was measured from the longest axis of the shell to determine the size distribution. The soft tissue weight was also recorded to assess the growth of this oyster. The condition factor (CF) was calculated to assess the general health condition and growth [15] using the following equation: $CF = 100W/L^3$, where W is the weight (g) and L is the total length (cm).

Shell size distribution and histological evaluation

The standard shell size distribution was determined using 50 samples per location. The sample *S. cucullata* specimens were immediately fixed after collection in 10% neutral buffered formalin fixative for 24 h at room temperature. The cross-sections were prepared using the dissected gonads, visceral mass, gills, and mantle tissues before decalcifying the exoskeleton with a decalcification medium. The histological blocks were prepared by the routine histopathological technique following the method of Howard et al [16]. The paraffin blocks were sectioned at $4 \mu\text{m}$ thickness with a rotary microtome and then stained with Masson's trichrome stain (MT) to observe the structural organization. The details of the histological slides were subjected to visual examination (Table S1, supplementary data) using a light microscope and scanned with

a PANORAMIC Digital Slide Scanner (3DHISTECH, Hungary).

Statistical analysis

The water quality parameters, morphometric observations, CF, the Msc density, and gametogenic histology data were represented as mean \pm SE. The unpaired t -test was used to compare these values between locations. The Msc and gametogenic histology data were subjected to Two-way ANOVA to determine statistical differences at $p < 0.05$ (GraphPad Prism for Windows version).

RESULTS

Water quality parameters

The water quality parameters including DO, pH, salinity, and turbidity were not significantly different between locations (Table 1). The water temperature at the DT was significantly higher than that at SB ($p < 0.05$).

Shell size distribution in relation to histological development

The shell size distribution of *S. cucullata* was classified into 5 groups based on the shell length: 1–2, 2.1–3, 3.1–4, 4.1–5, and 5.1–6 cm (Table 2). The oysters from the SB area were generally smaller than those from the DT site (Table 2). The highest and lowest mean CF were found in the size group of 1–2 cm (6.31 ± 1.67) and 5.1–6 cm (0.95 ± 0.48), respectively, from DT site (Table S2, supplementary data). In the size groups of 2.1–3 to 4.1–5 cm, the mean CF were higher in individuals from SB than those from the DT site. Several organs, including the digestive gland, gills, and mantle epithelium tissue, were histologically identified (Fig. 1A).

The digestive gland (or hepatopancreatic tissue) was composed of several blind-ended tubules, each of which could be divided into the primary and secondary ducts (Fig. 1B). The primary ducts were connected to the stomach wall (Fig. 1B). The smallest primary ducts were $105.4 \pm 3.03 \mu\text{m}$ in the 1–2 cm size group, and the largest were $139.9 \pm 3.63 \mu\text{m}$ in the 5.1–6 cm size group. Both sizes were observed in *S. cucullata* from the DT site. However, there were no significant differences in the average diameter of the primary and secondary ducts between *S. cucullata* from the 2 locations.

The gill structure of *S. cucullata* was made of V-shaped demi-branches, which were separated by the central axis (Fig. 1C). Each short gill filament extended toward either side of the axis, and the cilia observed on their surfaces were to produce the respiratory current (Fig. 1C). The gill filaments were divided into 2 rows and 3 zones, including the frontal, intermediate, and abfrontal zones (Fig. 1C). The anterior surface of the gill filament was covered with the cilia

Table 1 The environmental factors between the sampling sites.

Environment factor	Stone Bridge	Dugong Tourism by Drones	Standard range [16]
	mean \pm SE	mean \pm SE	
Dissolved Oxygen (mg/l)	6.46 \pm 0.49	6.35 \pm 0.42	>5 mg/l
Water temperature ($^{\circ}$ C)	31.71 \pm 0.07*	33.73 \pm 0.90*	25–30 $^{\circ}$ C
pH	8.26 \pm 0.37	8.85 \pm 0.24	6.5–9.0
Salinity (ppt)	31.13 \pm 0.15	31.47 \pm 0.07	20–30 ppt
Turbidity (NTU)	0.00	22.67 \pm 4.52	40 NTU
Depth (m)	0.88 \pm 0.09	0.78 \pm 0.12	–

Values are represented as mean \pm SE ($n = 3$). Significant differences between 2 locations (* $p < 0.05$). SE, standard error; ppt, part per thousand; and NTU, nephelometric turbidity unit.

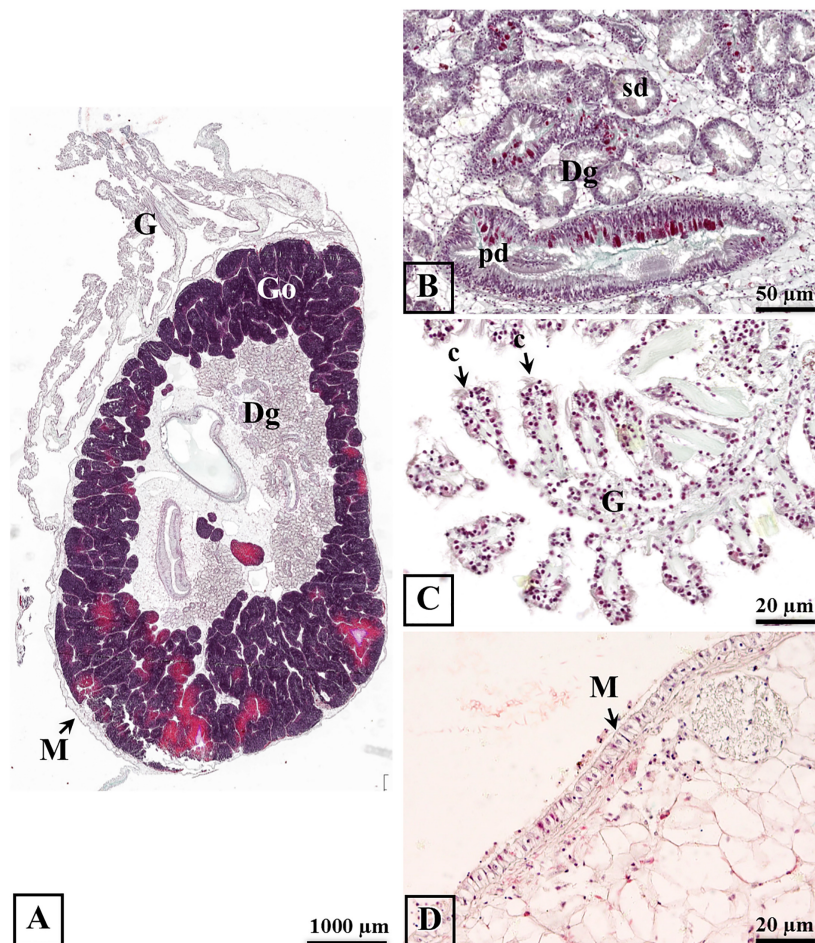


Fig. 1 Histological observations of different tissues of *S. cucullata*. The cross-section of *S. cucullata* showing the position of the digestive gland, gills, and mantle epithelium tissue (A). Digestive gland histology showing the primary and secondary ducts (B). Gill filaments extending toward the side and the cilia observed on their surface (C). The mantle layer in the vesicle mass with the connective tissue (D). Abbreviations: Dg, Digestive gland; pd, primary ducts; sd, secondary ducts; G, Gills; c, cilia; M, Mantle; and Go, Gonad.

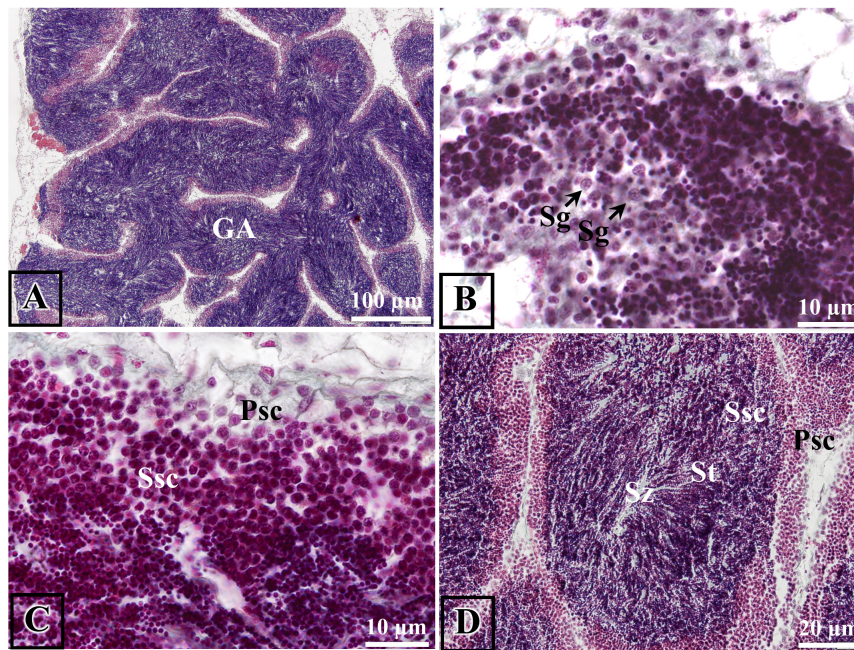


Fig. 2 Light microscope observation of the male gonad of *S. cucullata*. The spermatogenesis observed in the visceral mass. The mature gonad in gonadal acini (GA) (A) and spermatogonia (arrow) (B). The gonadal acini containing primary and secondary spermatocytes, Spermatids, and spermatozoa (C, D); Abbreviations: Sg, Spermatogonia; Psc, Primary spermatocytes; Ssc, Secondary spermatocytes; St, Spermatids; and Sz, Spermatozoa.

Table 2 Morphometric measurement based on the different sizes of the *S. cucullata* between the SB and the DT sites.

Size	Stone Bridge			Dugong Tourism by Drones		
	Diameter of digestive tubule (μm)	Length of gill (μm)	Length of mantle epithelium (μm)	Diameter of digestive tubule (μm)	Length of gill (μm)	Length of mantle epithelium (μm)
1-2 cm	-	-	-	105.4 ± 3.03	152.3 ± 5.46	31.24 ± 3.03
2.1-3 cm	120.9 ± 3.18	127.8 ± 3.29***	45.27 ± 3.18	121.9 ± 3.81	192.1 ± 3.92***	43.62 ± 3.81
3.1-4 cm	126.9 ± 2.66	145.7 ± 4.33**	45.51 ± 2.66	112.8 ± 2.98	157.0 ± 3.21**	45.05 ± 2.98
4.1-5 cm	129.3 ± 2.93	181.2 ± 8.45	60.72 ± 2.93***	133.0 ± 3.08	172.2 ± 5.62	73.78 ± 3.08***
5.1-6 cm	-	-	-	139.9 ± 3.63	280.2 ± 7.90	67.07 ± 3.63

Values are represented as mean ± SE (n = 6). Significant differences between the SB and the DT sites (** p < 0.01; *** p < 0.0001).

Table 3 Oocyte development in 4 stages of *S. cucullata* between 2-site study.

Size	Number of individual	Stone Bridge				Dugong Tourism by Drones			
		Oogonium (cells)	Immature oocyte (cells)	Maturing oocyte (cells)	Mature oocyte (cells)	Oogonium (cells)	Immature oocyte (cells)	Maturing oocyte (cells)	Mature oocyte (cells)
1-2 cm	6	-	-	-	-	-	-	-	-
2.1-3 cm	6	5.33 ± 1.76	5.00 ± 1.00	5.67 ± 1.20	7.67 ± 1.20	6.67 ± 2.40	1.33 ± 0.33	0	0
3.1-4 cm	6	3.33 ± 0.88	6.00 ± 1.73	6.33 ± 2.91	1.67 ± 1.20	5.33 ± 3.33	9.00 ± 1.73	5.00 ± 0.58	6.00 ± 1.16
4.1-5 cm	6	2.00 ± 1.16	9.67 ± 2.33	9.00 ± 0.58	10.67 ± 1.76	1.33 ± 0.33	2.67 ± 0.88	2.67 ± 0.88	4.67 ± 0.88
5.1-6 cm	6	-	-	-	-	2.33 ± 0.33	3.33 ± 0.88	5.33 ± 2.02	7.67 ± 1.76

Values are represented as mean ± SE (n = 6). No significant difference between the SB and the DT sites (p > 0.05).

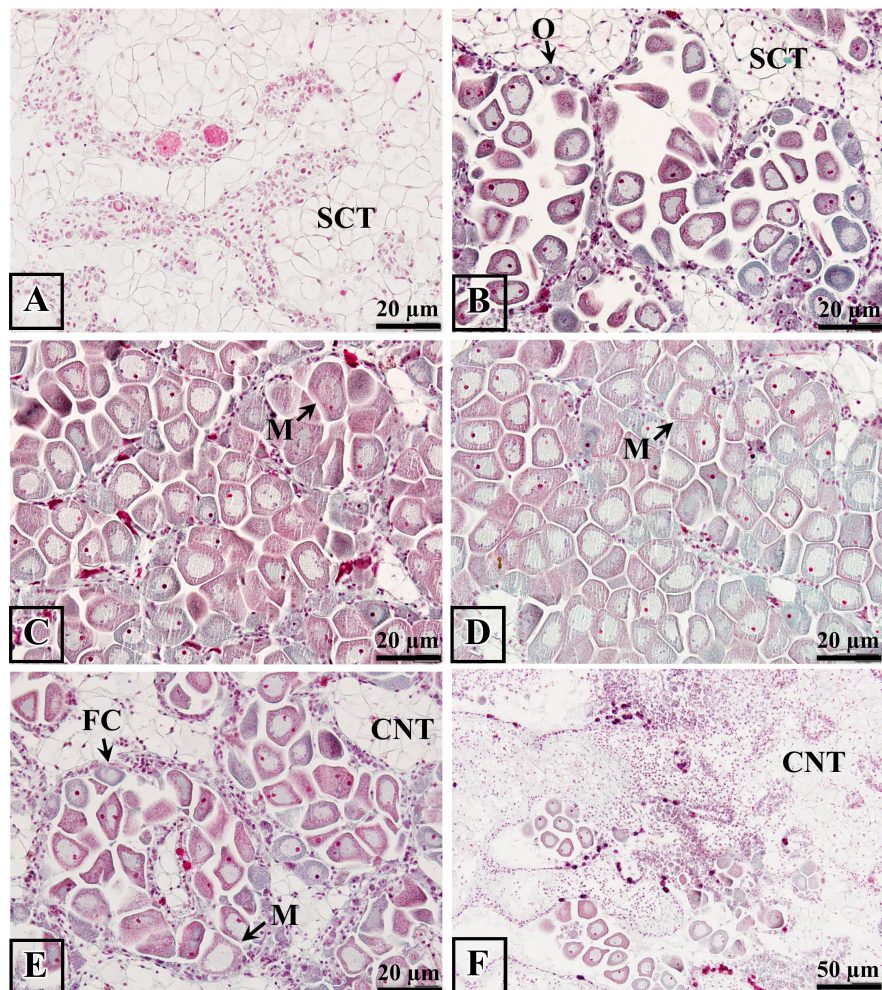


Fig. 3 Light microscope showing the female gonad development of the *S. cucullata* in follicle. Oocytes in pre-maturation stage with immature oocytes that stored connective tissue (A). Mature oocytes found in the follicles (B). The mature stage containing many mature oocytes with the absence of the interstitial tissue (C, D). Mature oocytes in the spent stage surrounded by follicular cells (E, F). Abbreviations: SCT, Storage Connective Tissue; FC, Follicular Cells; O, oogonium; M, mature oocyte; and CNT, Connective Tissue.

(Fig. 1C). The longest gill lamellae were observed in *S. cucullata* from the DT site ($280.2 \pm 7.90 \mu\text{m}$ in the 5.1–6 cm size group), whereas the shortest counterparts were recorded in the 3.1–4 cm group from SB ($127.8 \pm 3.29 \mu\text{m}$, Table 2). It was interesting that the mean lengths of the gill lamellae were significantly different between locations (Table 2).

The mantle of *S. cucullata* was covered with the vesicle mass, which histologically consists of 2 epithelium layers including outer epithelium and inner epithelium separated by haemolymph sinuses and connective tissues (Fig. 1D). Both the thickest ($31.24 \pm 3.03 \mu\text{m}$ in the 1–2 cm group) and thinnest ($73.78 \pm 3.08 \mu\text{m}$ in the 4.1–5 cm group) mantle epithelia were found in *S. cucullata* from DT (Table 2). The lengths of mantle epithelium were significantly

different between the 4.1–5 cm size groups from the 2 locations (Specific *F* value = 0.8605, $p < 0.0001$).

The gonadal follicles contained reproductive cells and were developed in the vesicle mass (Fig. 2A). The gonads of the *S. cucullata* samples were protandric from the 1–2 cm size group (Table S5, supplementary data). The male gonads were first formed with the blind-end testicular follicles containing spermatogonia (46.0 ± 24.54 cells of 2.1–3 cm at SB) (Fig. 2B, Table S5, supplementary data). Primary and secondary spermatocytes, spermatids, and spermatozoa were also identified in the 1–2 cm size group from SB (Fig. 2C–Fig. 2D, Table S5, supplementary data), and there was a tendency that male reproductive cells were more differentiated in larger size groups (Table S5, supplementary data). No significant differences in the

number of spermatogenic cells were found between *S. cucullata* from the SB and the DT sites.

Undeveloped female gonads were observed in the 1–2 cm size group. The ovary was histologically surrounded by a thin acinal wall and contained developing oocytes (Fig. 3A-B), which were classified into oogonia, immature oocytes, maturing oocytes, and mature oocytes (Table S4, supplementary data). Oogonia was prominently observed in the 2.1–3 cm size group (6.67 ± 2.40 cells) from the DT site (Fig. 3B, Table 3). Immature oocytes had a polyhedral-shaped nucleolus at the peripheral area (9.67 ± 2.33 cells of 4.1–5 cm at the SB site) (Table 3). The mature oocytes had a polyhedral-shaped voluminous nucleus surrounded by the basophilic cytoplasm (9.0 ± 0.58 cells of 4.1–5 cm at the SB site) (Fig. 3C-D, Table 3) and completed in the spent stage. The development of mature oocytes was still seen, but the stromal compartment and the loose connective tissue were also increased (Fig. 3E-F, Table 3). However, no statistically significant differences in ovarian activity were found between *S. cucullata* from both sites.

Overall, *S. cucullata* individuals were primarily asexual in the smallest size group of 1–2 cm. The protandric characteristic appeared in the 2.1–3 cm and 3.1–4 cm size groups with observed sexes of female, male, and hermaphrodites. All *S. cucullata* individuals in the 4.1–5 cm size group from DT site were female (Table S3, supplementary data).

Distribution of mucous-secreting cells

The Msc of *S. cucullata* were variously oval, cup-like, stick-like, and pear-like shapes (Fig. 4A). In the gill lamellae, the Msc with stick-like and cup-like shapes were observed (Fig. 4B). The digestive ducts contained the oval and cup-like shapes (Fig. 4C), and the mantle epithelium contained oval and pear-shaped Msc (Fig. 4D). The cup-like and oval-shaped cells were predominant (Fig. 4C), especially in the 3.1–4 cm size group from the SB site (65.0 ± 44 cells).

Our investigation showed that increases in Msc were usually identified in the gill lamellae that had oval, cup-like, and pear-like shapes (Fig. 4B). The density of Msc was lower in the *S. cucullata* 4.1–5 cm size group from the SB site (13.75 ± 9.20 cells) than in the same size group from the DT site (37.50 ± 34.18 cells). We observed in the size group of 3.1–4 cm for *S. cucullata* that its highest density of Msc from the SB site (65.0 ± 44.75 cells) was in the digestive gland but the highest density of Msc was in the mantle epithelium (24.25 ± 11.32 cells) from the DT site. The smallest and largest Msc were recorded in the 4.1–5 cm size group from both locations (Table 4). Overall, our observation showed that the features of Msc were not significantly different between the 2 locations (Table 4).

DISCUSSION

Between the 2 sampling locations, only the water temperature was significantly different. This might be related to the fact that the sampling sites were in the intertidal zone, where the water temperatures vary depending on the season. Temperatures are higher in summer; therefore, the seasonal effect will be bigger in the shallow areas [17]. We suggest that this difference in water temperature might be responsible for the observed differences in condition factors and reproductive activity of the oysters [18]. Indeed, Rajapandian et al [19] showed that the water temperature correlated with the CF in *Crassostrea madrasensis* with the highest CF in April. These results were consistent with other previous observations in *Pinctada margaritifera* [18] and *Crassostrea gigas* [20].

The morphometric characteristics of the *S. cucullata* specimens from the SB site were smaller than those from the DT site. Since the tested parameters such as CF are closely related to the available food in oysters [15], the DT site might represent a more favorable environment for *S. cucullata* than the SB site. It is noted that the DT site is located near the seagrass beds which grow more prolifically in the higher sediment areas with higher nutrients which comprise an important and diverse habitat and play a significant role in the growth and abundance of suspension-feeding bivalves [11, 21]. The high growth and CF have been associated with the feeding activity in *Hemifusus ternatanus* under artificial conditions [22] and *Pinctada margaritifera var erythraensis* collected from Dongonab Bay, Red Sea, Sudan [23].

The structures of the digestive gland, gills, gonads, and mantle of *S. cucullata* are similar to those in other bivalves such as *Pecten maximus* [24] and *Crassostrea gigas* [25]. Interestingly, the length of the gill lamellae and mantle of the specimen *S. cucullata* showed significant differences between the 2 sampling locations. This might be related to the different rates of development since these organs are involved in respiration and feeding [26]. It was reported in Cannuel and Beninger [27] that gill development in *Crassostrea gigas* juveniles rapidly developed to increase food-feeding efficiency.

In our study, we also showed that *S. cucullata* has protandric characteristics with no statistically significant differences in the gonadal development between the 2 locations. It might be noted that the protandrous hermaphrodites of oysters normally occur in various periods including the first spawning period and when changing sex to spawn as females [28] as in *Modiolus capax* [29] and *Crassostrea brasiliiana* [30]. The male gonad began to develop in the 1–2 cm size group, whereas the female gonad began to develop in the 2.1–3 cm size group, which corresponds to the juvenile stage. This indicates the oysters started life as male and subsequently changed permanently into

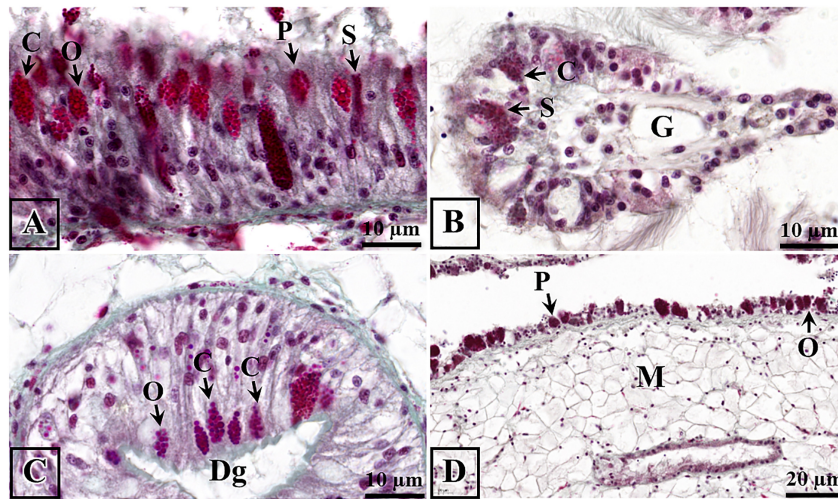


Fig. 4 The light microscope of mucous-secreting cells of the *S. cucullata*. Masson trichome staining. The cross section of *S. cucullata* presenting mucous-secreting cells in 4 types (A). Mucous cells in gill filament with cup-like and stick-like shapes (arrow) (B); the secondary digestive tubules showing mucous cells of oval and cup-like shapes (arrow) (C). Mantle epithelium cells showing the large mucous cell (D). Abbreviations: O, Oval or circle-like; C, cup-like; S, Stick-like; and P, Pear-like.

Table 4 Density of mucous-secreting cells in three tissue of the *S. cucullata* between the SB and the DT sites.

Size	Stone Bridge			Dugong Tourism by Drones		
	Digestive gland (cells)	Gill (cells)	Mantle epithelium (cells)	Digestive gland (cells)	Gill (cells)	Mantle epithelium (cells)
1–2 cm	–	–	–	37.00 ± 20.88	26.00 ± 17.87	9.75 ± 5.53
2.1–3 cm	32.50 ± 24.52	15.75 ± 11.81	9.00 ± 4.56	23.25 ± 8.34	35.75 ± 28.24	17.00 ± 9.55
3.1–4 cm	65.00 ± 44.75	20.75 ± 12.29	6.25 ± 3.71	25.25 ± 13.46	20.25 ± 9.39	18.00 ± 8.85
4.1–5 cm	27.25 ± 13.15	13.75 ± 9.20	5.75 ± 2.75	39.75 ± 27.93	37.50 ± 34.18	24.25 ± 11.32
5.1–6 cm	–	–	–	19.00 ± 10.66	36.50 ± 21.64	7.75 ± 4.51

Values are represented as mean ± SE ($n = 6$). No significant difference between the SB and the DT sites ($p > 0.05$).

female after about a year or when they increased in size. Similar gonadal maturation patterns have been found in other bivalves including *Crassostrea glomerata* [28], *Crassostrea corteziensis* [31], and *Haliotis discus hannai* [32]. The beginning of the adult stage was when the size of 4.1–5 cm was attained like other bivalves such as *Crassostrea gigas* [33] and *Crassostrea iredalei* [34].

The Msc of the *S. cucullata* oyster specimens had oval, cup-like, and pear-like shapes, which is similar to the findings in *Haliotis diversicolor* [35], *Solen grandis Dunker* [36], *Chaetopleura angulate*, and *Acanthochitona fascicularis* [37]. Msc is essential to marine molluscs in producing various functional substances together with glands in the epithelium that produce exudate. The highest density of Msc was observed in the digestive gland, suggesting that it is the main organ for mucus production. This is similar to the findings of Yonge [38] and indicates that the mucus in the digestive organs has various roles including food,

locomotion, and immunity activity [39,40]. The maximum density of the *S. cucullata* specimens' Msc was observed in the 3.1–4 cm size group, and a dramatic decrease in Msc was observed in the 4.1–5 cm size group. This might be related to the environmental situation but requires further investigation.

CONCLUSION

The histological observations of *S. cucullata* from Li-bong Island identified their juvenile (<4 cm) and adult (>4 cm) stages by the size of their organs, including the digestive gland, gills, and mantle. The histological observations also showed the size at sexual maturation, at which gametogenesis begins, although this is influenced by environmental conditions and available nutrients. The density and morphology of the Msc may serve as good biomarkers to assess the health and immune function of *S. cucullata*, particularly in different-sized population distributions.

Appendix A. Supplementary data

Supplementary data associated with this article can be found at <http://dx.doi.org/10.2306/scienceasia1513-1874.2023.095>.

Acknowledgements: This research was supported by a scholarship for Honors Graduates in the master's courses in the Faculty of Medical Sciences, Naresuan University (NU). The preparation of samples was completed in the Marine Natural Product Laboratory of the Faculty of Science and Fisheries Technology, Rajamangala University of Technology, Srivijaya Trang Campus. All further preparation and analysis processes were completed in the Department of Anatomy, Faculty of Medical Science, NU. The authors wish to thank Mr. Roy I. Morien of the NU Graduate School for his editing of the grammar, syntax, and general English expression in this manuscript.

REFERENCES

- Bourassa N, Morin A (1995) Relationships between size structure of invertebrate assemblages and trophy and substrate composition in streams. *J North Am Benthol Soc* **14**, 393–403.
- Fey F, Dankers N, Steenbergen J, Goudswaard K (2009) Development and distribution of the non-indigenous Pacific oyster (*Crassostrea gigas*) in the Dutch Wadden Sea. *Aquac Int* **18**, 45–59.
- Kang D, Chu FE, Yang H, Lee C, Koh H, Choi K (2010) Growth, reproductive condition, and digestive tubule atrophy of Pacific oyster *Crassostrea gigas* in Gamakman Bay off the Southern Coast of Korea. *J Shellfish Res* **29**, 839–845.
- Davenel A, González R, Suquet M, Quéllec S, Robert R (2010) Individual monitoring of gonad development in the European flat oyster *Ostrea edulis* by *in vivo* magnetic resonance imaging. *Aquac* **307**, 165–169.
- Loor A, Sonnenholzner S (2016) Reproductive cycle of the rock oyster, *Striostrea prismatica* (Gray, 1825) from two locations on the southern coast of Ecuador. *Aquac Res* **47**, 1432–1442.
- Wang Y, Zhang H, Fodjo EK, Kong C, Gu R, Han F, Shen X (2018) Temperature effect study on growth and survival of pathogenic *Vibrio parahaemolyticus* in Jinjiang oyster (*Crassostrea rivularis*) with rapid count method. *J Food Qual* **2018**, 2060915.
- Arkhipkin AI, Boucher E, Gras M, Brickle P (2017) Variability in age and growth of common rock oyster *Saccostrea cucullata* (Bivalvia) in Ascension Island (central-east Atlantic). *J Mar Biol Assoc* **97**, 735–742.
- Sampantamit T, Ho LT, Lachat C, Sutumawong N, Sorgeloos P, Goethals P (2020) Aquaculture production and its environmental sustainability in Thailand: Challenges and potential solutions. *Sustain* **12**, 2010.
- Thanormjit K, Chueycham S, Phrprasert P, Sukparangsi W, Kingtong S (2020) Gamete characteristics and early development of the hooded oyster *Saccostrea cucullata* (Born, 1778). *Aquac Rep* **18**, 100473.
- Wang T, Li Q (2018) Effects of salinity and temperature on growth and survival of juvenile Iwagaki oyster *Crassostrea nippona*. *J Ocean Univ China* **17**, 941–946.
- Kobkeathawin T, Sirivithayapakorn S, Nitiratsuwat T, Muenhor D, Loh PS, Pradit S (2021) Accumulation of trace metal in sediment and soft tissue of *Strombus canarium* in a tropical remote island of Thailand. *J Mar Sci Eng* **9**, 991.
- Cardoso IDS, Alves ECS, Rodrigues L, Guedes AL, De Oliveira LC, De Quadros MLA, Da Silva FNL (2021) Can the *Ucides cordatus* fishing and the *Crassostrea Gasar* creation on the Amazon Coast make up the curriculum of rural schools. *J Fish Sci* **3**, 37–46.
- Wilson JM, Bunte RM, Carty A (2009) Evaluation of rapid cooling and tricaine methanesulfonate (MS222) as methods of euthanasia in zebrafish (*Danio rerio*). *J Am Assoc Lab Anim Sci* **48**, 785–789.
- OIE (2021) *Diseases of Mollusc Manual of Diagnostic Tests for Aquatic Animals*, OIE representation for Asia and the Pacific. Tokyo, Japan.
- Lim L, Liew K, Yap T, Tan N, Shi C (2020) Length-weight relationship and relative condition factor of pearl oyster, *Pinctada fucata martensii*, cultured in the Tieshangang Bay of the Beibu Gulf, Guangxi Province, China. *Borneo J Mar Sci Aquac* **4**, 24–27.
- Howard DW, Keller BJ, Lewis EJ, Smith CS (2004) *Histological Techniques for Marine Bivalve Mollusks and Crustaceans*, Amsterdam, The Netherlands, pp 59–79.
- Rybovich M, La PMK, Hall SJ, La PJF (2016) Increased temperatures combined with lowered salinities differentially impact oyster size class growth and mortality. *J Shellfish Res* **35**, 101–113.
- Latchere O, Mehn V, Gaertner-Mazouni N, Moullac GL, Fievet J, Belliard C, Saulnier D (2018) Influence of water temperature and food on the last stages of cultured pearl mineralization from the Black-lip pearl oyster *Pinctada margaritifera*. *PLoS One* **13**, e0193863.
- Rajapandian ME, Gopinathan CP, Rodrigo JX, Gandhi AD (1990) Environmental characteristics of edible oyster beds in and around Tuticorin. *J Mar Biol Assoc India* **32**, 90–96.
- Kim AC, Lozhkin DV (2021) Influence of total water-temperature value on the size and weight characteristics of Pacific oyster *Crassostrea gigas* (Thunberg, 1793) in the Aniva Bay (Sakhalin Island) according to Satellite data. *Izv Atmos Ocean Phys* **57**, 1712–1719.
- Luesiri M, Boonsanit P, Lirdwitayaprasit T, Pairohakul S (2022) Filtration rates of the green-lipped mussel *Perna viridis* (Linnaeus, 1758) exposed to high concentration of suspended particles. *ScienceAsia* **48**, 452–458.
- Yang S, Cheng F, Wu X, Xing Y, Gu Z, Tang X (2020) Length-weight relationship and growth of a marine gastropod mollusk, *Hemifusus ternatanus* (Gmelin) (Family: Melongenidae). *Pakistan J Zool* **52**, 2027–2426.
- Elamin M, Eldin ME (2015) Productivity and economic values of the pearl oyster (*Pinctada margaritifera var erythraensis*) cultured in Dongonab Bay, Red Sea. *Int J Sci Environ Technol* **1**, 1193–1204.
- Beninger PG, Dwiono SAP, Pennec ML (1994) Early development of the gill and implications for feeding in *Pecten maximus* (Bivalvia: Pectinidae). *Mar Biol* **119**, 405–412.
- Dutertre M, Ernande B, Haure J, Barillé L (2017) Spatial and temporal adjustments in gill and palp size in the oyster *Crassostrea gigas*. *J Molluscan Stud* **83**, 11–18.
- Zhang X, Ye B, Gu Z, Liu L, Yang S, Wang A, Liu C (2021) Comparison in growth, feeding, and metabolism between a fast-growing selective strain and a cultured population of pearl oyster (*Pinctada fucata martensii*).

- Front Mar Sci* **8**, 1–9.
27. Cannuel R, Beninger PG (2006) Gill development, functional and evolutionary implications in the Pacific oyster *Crassostrea gigas* (Bivalvia: Ostreidae). *Mar Biol* **149**, 547–563.
 28. Dinamani P (1974) Reproductive cycle and gonadial changes in the New Zealand rock oyster *Crassostrea glomerata*. *NZ J Mar Freshwater Res* **8**, 39–65.
 29. García-Corona JL, Rodríguez-Jaramillo C, Saucedo PE, López-Carvallo JA, Arcos-Ortega GE, Mazón-Suástegui JM (2018) Internal energy management associated with seasonal gonad development and oocyte quality in the horse mussel *Modiolus capax* (Bivalvia: Mytilidae). *J Shellfish Res* **37**, 475–483.
 30. Castilho-Westphal G, Magnani F, Ostrensky A (2015) Gonad morphology and reproductive cycle of the mangrove oyster *Crassostrea brasiliensis* (Lamarck, 1819) in the baía de Guaratuba, Paraná, Brazil. *Acta Zool* **96**, 99–107.
 31. Rodríguez-Jaramillo C, Hurtado MÁ, Romero-Vivas E, Ramírez J, Manzano M, Palacios E (2008) Gonadal development and histochemistry of the tropical oyster, *Crassostrea corteziensis* (Hertlein, 1951) during an annual reproductive cycle. *J Shellfish Res* **27**, 1129–1141.
 32. Awaji M, Hamano K (2004) Gonad formation, sex differentiation and gonad maturation processes in artificially produced juveniles of the abalone, *Haliotis discus hannai*. *Aquac* **239**, 397–411.
 33. Mizuta D, Júnior NS, Fischer C, Lemos D (2012) Interannual variation in commercial oyster (*Crassostrea gigas*) farming in the sea (Florianópolis, Brazil, 27°44' S; 48°33' W) in relation to temperature, chlorophyll a and associated oceanographic conditions. *Aquac* **366–367**, 105–114.
 34. Chueachat P, Tarangkoon W, Tanyaros S (2018) A comparative study on the nursery culture of hatchery-reared sub-adult cupped oyster, *Crassostrea iredalei* (Faustino, 1932), in an earthen pond and a mangrove canal. *Fish Aquatic Sci* **26**, 217–222.
 35. Di G, Ni J, Zhang Z, You W, Wang B, Ke C (2012) Types and distribution of mucous cells of the abalone *Haliotis diversicolor*. *Afr J Biotechnol* **11**, 9127–9140.
 36. Xiuzhen S, Wenbin Z, Sulian R (2003) Structure and function of the digestive system of *Solen grandis* Dunker. *J Ocean Univ China* **2**, 155–159.
 37. Lobo-Da-Cunha A, Alves Â, Oliveira E, Calado G (2022) Functional histology and ultrastructure of the digestive tract in two species of chitons (Mollusca, Polyplacophora). *J Mar Sci Eng* **10**, 160.
 38. Yonge CM (1926) Structure and physiology of the organs of feeding and digestion in *Ostrea edulis*. *J Mar Biolog Assoc UK* **14**, 295–386.
 39. Allam B, Carden WE, Ward JJ, Ralph GM, Winnicki SM, Espinosa EP (2013) Early host-pathogen interactions in marine bivalves: Evidence that the alveolate parasite *Perkinsus marinus* infects through the oyster mantle during rejection of pseudofeces. *J Invertebr Pathol* **113**, 26–34.
 40. Zhang Y, Qin Y, Ma L, Zhou Z, Xiao S, Ma H, Yu Z (2019) Gametogenesis from the early history life stages of the kumamoto oyster *Crassostrea sikamea* and their breeding potential evaluation. *Front Physiol* **10**, 1–8.

Appendix A. Supplementary data

Table S1 Histological characteristics of the *S. cucullata* observed in this study.

Organ/Cell	Morphometric description	Reference
Gill filament	The length of the gill lamellae from base to apex ($n = 50$ per individual sample of size distribution)	Yonge [37]
Mantle epithelium	The mantle epithelium ($n = 50$ per individual sample of size distribution)	
Digestive tubule	The diameter of primary ducts ($n = 50$ per individual sample of size distribution)	
Mucous-secreting cell (Msc)	Types of mucous-secreting cell: oval, cup-shaped, pear-shaped, stick-shaped	Di et al [34]
Gametogenic cell and tissue	Types of germ cells: male, female, hermaphrodites, or asexual reproductive patterns	Zhang et al [39]
	Gametogenesis and gonadal maturation	García-Corona et al [28]
	Oogenic differentiation	Castilho-Westphal et al [29]

Table S2 The condition factor (g/cm^3) of the sampled *S. cucullata* between the SB and the DT sites.

Size distribution	Number of individual	Stone Bridge	Dugong Tourism by Drones
		mean \pm SE	mean \pm SE
1–2 cm	10	–	6.31 \pm 1.67
2.1–3 cm	10	4.25 \pm 2.18	2.01 \pm 0.82
3.1–4 cm	10	3.93 \pm 1.41	2.16 \pm 0.68
4.1–5 cm	10	2.01 \pm 0.46	1.27 \pm 0.45
5.1–6 cm	10	–	0.95 \pm 0.48

Values are represented as mean \pm SE ($n = 10$); SE, standard error.

Table S3 Percentage of sex difference of the *S. cucullata* between 2 locations.

Size	Number of individual	Stone Bridge				Dugong Tourism by Drones			
		Female	Male	Hermaphrodite	Asexual	Female	Male	Hermaphrodite	Asexual
1–2 cm	6	–	–	–	–	–	16.67%	–	83%
2.1–3 cm	6	50%	50%	–	–	50%	33.33%	–	16.67%
3.1–4 cm	6	50%	16.67%	33.33%	–	50%	33.33%	16.67%	–
4.1–5 cm	6	66.67%	16.67%	16.67%	–	100%	–	–	–
5.1–6 cm	6	–	–	–	–	100%	–	–	–

Table S4 The characteristics of spermatogenesis stage and oogenesis stage of the *S. cucullata*.

Stage	Cell	Description
Spermatogenesis		
1	Spermatogonium	Large nucleus with distributed chromatin inside the cell
2	Spermatocyte	The nucleus condenses in the primary phase and through cell division in the secondary phase
3	Spermatid	Occurs from meiosis division in half of the genetic material of the previous cell, resulting in a reduced cells size and more compacted nuclei
4	Spermatozoon	Characterized by long flagella
Oogenesis		
1	Oogonium	The cytoplasm is reduced to the size of the nucleus of the basophil cell.
2	Immature oocyte	Basophils usually have a peripheral polyhedral-shaped nucleolus
3	Maturing oocyte	Lightly eosinophilic, polyhedral-shaped voluminous nucleus
4	Mature oocyte	Eosinophilic, voluminous nucleus, located near the follicle lumen

Table S5 Type of male gonad of the *S. cucullata* from the SB and the DT sites.

Location	Size distribution	Number of individual	Spermatogenesis stage				
			Spermatogonium (cells)	Primary spermatocyte (cells)	Secondary spermatocyte (cells)	Spermatid (cells)	Spermatozoon (cells)
Stone	2.1–3 cm	6	46.0 ± 24.54	434.67 ± 82.96	272.0 ± 161.7	632.0 ± 378.60	524.7 ± 412.6
Bridge	3.1–4 cm	6	6.67 ± 4.18	103.3 ± 59.83	230.3 ± 126.0	216.7 ± 18.98	506.7 ± 45.08
	4.1–5 cm	6	9.67 ± 3.76	479.3 ± 88.37	602.0 ± 192.3	559.7 ± 126.4	1306.0 ± 295.4
Dugong	1–2 cm	6	12.67 ± 5.24	49.33 ± 3.67	49.67 ± 6.69	40.33 ± 9.94	15.33 ± 5.04
Tourism	2.1–3 cm	6	19.67 ± 0.67	133.7 ± 29.36	145.7 ± 43.35	292.3 ± 72.26	143.7 ± 23.84
by Drones	3.1–4 cm	6	9.67 ± 5.21	177.7 ± 45.04	301.7 ± 179.0	345.0 ± 183.0	201.0 ± 54.67

Values are represented as mean ± SE ($n = 6$). No significant difference between the SB and the DT sites ($p > 0.05$).